A Diverse Benchmark Based on 3D Matched Molecular Pairs for Validating Scoring Functions

Lena Kalinowsky[1] [‡], Julia Weber[1] [‡], Shantheya Balasupramaniam[2], Knut Baumann[2] and Ewgenij Proschak[,1].*

1. Institute of Pharmaceutical Chemistry, Goethe University Frankfurt, Max-von-Laue Str. 9, Frankfurt a.M., D-60438 Germany.

2. Institute of Medicinal and Pharmaceutical Chemistry, Technical University of Braunschweig, Beethovenstr. 55, Braunschweig, D-38106 Germany.

The 13 scoring functions evaluated in this study are briefly described below. A detailed description of the scoring functions can be found in the cited references.

(1) **MOE.** The commercially available software MOE 2014.09[1] provides four empirical scoring functions (London dG, ASE, Affinity dG, Alpha HB) and one force-field scoring function (GBVI/WSA dG).

(1.1) **London dG/MOE.** London dG estimates free binding energy of ligands using a set of energy and assessment terms. Those include hydrogen and metal bond geometries, rotation and translation entropy as well as solvation energy contributions.

(1.2) **ASE/MOE.** ASE accumulates the Gaussian function of all atom-receptor pairs and Atom-Alpha HB sphere pairs of each complex.

(1.3) **Affinity dG/MOE.** Affinity dG uses a linear function to calculate the enthalpy contribution to the binding free energy (G).

(1.4) **Alpha HB/MOE.** Alpha HB uses a linear combination of two terms. One term comprises the geometric fit of the ligand to the binding site. The other term comprises hydrogen bond effects.

(1.5) **GBVI/WSA dG/MOE.** The force-field scoring function GBVI/WSA dG was trained at the MMFF94x[2] and AMBER99 force-field[3–5] using the SIE (solvated interaction energy) training data set.[6] It estimates the free binding energy with weighted terms for the Coulomb energy, solvation energy and van-der-Waals contributions.

(2) **GOLD.** The genetic algorithm GOLD (genetic optimization for ligand docking) is available in the software package GOLD Suite 5.2.2.[7–14] The package provides two empirical scoring functions (ChemPLP and ChemScore), one knowledge-based scoring function (ASP) and one force-field scoring function (GoldScore).

(2.1) **ChemPLP/GOLD.** The ChemPLP scoring function combines parameter from the ChemScore (distance and angle dependences of hydrogen and metal bonds) and PLP (Piecewise

Linear Potential) scoring function (heavy-atom-collision and torsion potentials, covalent bond contributions, protein sidechain flexibility and optional constrains).[11]

(2.2) **ChemScore/GOLD.** The empirical scoring function ChemScore was trained with experimental binding affinities. The function is composed of the binding free energy contribution as well as penalty values for collisions, internal torsions, covalent contributions and constrains (see ChemPLP).[12,13]

(2.3) **ASP/GOLD.** The ASP (Astex Statistical Potential) is a statistic atom-atom potential generated from statistical analysis of protein-ligand interactions found in the PDB.[10]

(2.4) **GoldScore/GOLD.** GoldScore as a force-field scoring function consists of four terms for hydrogen binding and van-der-Waals energy further intern van-der-Waals and torsion energies.[15]

(3) **AutoDock Tools.** The scoring functions AutoDock 4.2.6and AutoDock Vina 1.1.2 are provided by the software package AutoDock Tools.[16]

(3.1) **AutoDock 4.2.6.** AutoDock 4.2.6 is a semi-empirical, force-field scoring function which calculates pairwise interactions between protein and ligand. The surrounding water is evaluated with an empirical method. Both enthalpy and entropy contributions are about to be considered.[17]

(3.2) **AutoDock Vina 1.1.2.** AutoDock Vina 1.1.2 is a combination of a knowledge-based and empirical scoring function to consider the advantages of both scoring function types.[18]

(4) **X-Score.** X-Score is an empirical scoring function considering van-der-Waals interactions, hydrogen bridge bonds, entropy loss due to ligand binding, the hydrophobic effect and a regression constant considering the loss of enthalpy and entropy due to ligand btargetinding.[19]

(5)   **DSX.** DSX is a knowledge-based scoring function which composed of three weighted parts of a distance dependent pair-potential, a knowledge-based angel dependent torsion potential as well as a ratio of the solvent-accessible surface (SAS) from the bound and unbound state.[20]

Table S1. Detailed information regarding PDB codes, affinity data and target-protein name of the data set of 99 3D-MMPs.

Cluster_ID	ID_pair (L/R)	Affinity_L [μM]	Affinity_R [μM]		Target-protein name	Δaffinity
23	3HVH_3HVJ	0.003	0.002			0.18
	3OE4_3OZT	0.034	74.9	K_i	O-methyltransferase	-3.34
	3OZS_3OZT	4.645	74.9			-1.21
59	3SV2_3QX5	64	63.5			0.003
	2ZDA_3SI4	0.004	132.2	K_i	Thrombin	-4.52
	1QBV_3SV2	4.1	64			-1.19
83	3QU0_3QXP	0.02	0.02			0.0
	3R9H_3QXP	100	0.02	IC_{50}	CDK2	3.7
	2VTP_2VTT	0.003	0.044			-1.17
156	4JQ7_4JR3	0.393	0.218			0.26
	4JR3_4JQ8	0.218	0.008	IC_{50}	EGFR	1.44
	4JRV_4JQ8	0.029	0.008			0.56
167	4C38_4C37	0.0174	0.0197			-0.05
	2UW3_2UW4	80	5.2	IC_{50}	Protein Kinase A	1.19
	2OH0_2OJF	0.018	0.11			-0.79
194	3SWW_3SX4	0.004	0.003	K_i		0.12
	3OC0_3KWF	0.52	0.0068	IC_{50}	Human DPP-IV	1.88
	4LKO_4JH0	0.006	0.00094	K_i		0.81
324	2XPK_2J62	0.000005	0.0000046			0.04
	2WB5_2J62	0.00074	0.0000046	K_i	O-Glcnacase	2.21
	2WB5_2XPK	0.00074	0.000005			2.17
325	2CES_2J7E	0.056	0.048			0.07
	1OIF_2J75	0.019	0.225	K_d	Beta-Glucosidase	-1.07
	2J7G_2J7E	0.1	0.048			0.32
441	3EJQ_3EJR	0.0027	0.0027	K_i		0.0
	3DX1_2F7O	265	0.036		Golgi Alpha-Mannosidase II	3.87
	2F18_2F1B	80	1000	IC_{50}		-1.1
466	4H1E_4H3I	0.003	0.003	K_i		0.0
	4I0F_4I1C	0.45	0.008		BACE-1	1.75
	4JP9_4JPC	0.024	0.094	IC_{50}		-0.59
487	3UO5_3UP2	0.039	0.04	K_d		-0.01
	4DEA_3UP7	0.256	0.0061	IC_{50}	Aurora A	1.62
	3UNZ_3UOJ	0.016	0.051	K_d		-0.5
518	2ONZ_2OBF	0.0013	0.0014	K_i		-0.03
	3KR0_3KR1	20	1.8	K_d	hPNMT	1.05
	1N7J_1HNN	0.37	0.58	K_i		-0.2
686	3GE7_3EOS	0.002	0.004			-0.3
	1S39_1S38	0.02	7	K_i	tRNA-Guanine Transglycosylase	-2.54
	3V0Y_3RR4	4.1	28.05			-0.84
710	1LOQ_3WJW	200	134		Orotidine 5'-monophosphate decarboxylase (ODCase)	0.17
	3G1V_1LOR	645	0.0000088	K_i		7.87
	3G1V_1KM3	645	12.4			1.72
745	2VCJ_2VCI	0.021	0.021	IC_{50}	HSP90 Chaperone	0.0
	2XHX_2XHT	0.25	1.1	K_d		-0.64

	2YI0_2YI7	0.0075	0.0048			0.19
790	2XBX_2XBW	0.015	0.01			0.18
	2UWO_2UWP	0.002	0.154	K_i	Factor XA	-1.89
	2JKH_2Y5F	0.009	0.002			0.65
806	4DE3_4DDY	3	2.4			0.1
	4DE2_4DDY	76	2.4	K_i	CTX-M-9 class A beta-lactamase	1.5
	3G35_4DE3	21	3			0.85
810	1F8C_2QWE	0.04	0.033			0.08
	1F8E_1F8C	15	0.04	K_i	Influenza Neuraminidase	2.57
	1F8D_1F8B	400	4			2.0
812	3O9A_3O9D	0.00002	0.000019			0.02
	3O9B_3O9A	0.0000005	0.00002	K_i	HIV-1 Protease	-1.6
	4DJR_3O9D	0.000003	0.000019			-0.8
873	3IOC_3IOD	210	80		Mycobacterium Tuberculosis Pantothenate Synthetase	0.42
	3IUB_3IUE	29	1.5	K_d		1.29
	3COY_3COW	0.96	0.125			0.89
900	3NX7_3F15	0.00788	0.00788			0.0
	3LKA_3LK8	1500	0.0197	K_d	Human MMP12	4.88
	3LK8_3F15	0.0197	0.00788			0.4
914	2ZFS_2ZQ2	0.287	0.276	K_d		0.02
	1O35_1O3J	10	0.17	K_i	Serine Protease	1.77
	1TNK_1TNL	32500	13300			0.39
929	3E6K_3LP4	7	13.1			-0.27
	3F80_2AEB	60	0.005	K_d	Arginase I	4.08
	3SJT_3SKK	0.88	34			-1.59
942	1Q6J_1Q6M	0.016	0.013	IC_{50}		0.09
	2QBP_2NT7	0.004	0.3	K_i	Protein-tyrosine phosphatase 1b	-1.88
	2VEX_2VEW	0.18	0.064	IC_{50}		0.45
975	1NVR_1NVQ	0.0078	0.0056	K_i	Checkpoint Kinase 1 (CHK1)	0.14
	2XEZ_2XF0	1.5	30			-1.3
	2WMW_2WMX	0.39	0.86	IC_{50}		-0.34
979	1GI8_1GI9	8.9	6			0.17
	1OWE_1OWH	0.631	0.04	K_i	Urokinase	1.2
	1W0Z_1W11	0.021	0.006			0.54
1024	4EHV_4EH9	5103	5453	IC_{50}		-0.03
	3NNU_3NNW	0.048	0.009		P38 MAP kinase	0.73
	3GCU_3GCV	0.165	0.074	K_d		0.35
1025	3ZSQ_3ZSO	10.9	7.6	K_d		0.16
	3AV9_3AVB	435	85.2	IC_{50}	HIV type 1 integrase	0.71
	4CEB_3ZSW	1080	2000	K_d		-0.27
1050	3F3D_3F3E	0.069	0.02	K_d		0.54
	3F48_3F3E	0.512	0.02		LeuT	1.41
	2Q72_2Q6H	2090	250	IC_{50}		0.92
1051	1I9Q_1G48	0.0039	0.0039	K_d		0.0
	2H15_3HKU	2.135	0.005	K_i	Carbonic Anhydrase II	2.63
	3IBI_3IBU	0.0026	0.0007			0.57
1059	1MQH_1MQG	0.3	0.52			-0.24
	1MQJ_1MQI	4.76	0.02353	IC_{50}	GluR2	2.31
	1MQJ_1MQH	4.76	0.3			1.2
1072	1JVU_1O0M	7	7.1	K_i	Ribonuclease A	-0.01
	3DXG_3D6O	4000	77			1.72

	1O0H_1AFK	1.2	0.24			0.7
1081	3MRT_3MS2	200	192.4	IC_{50}	Glycogen phosphorylase b (GPb)	0.02
	4EL5_4EJ2	4.3	3204			-2.87
	3SYR_3T3H	7.9	1.94	K_i		0.61

Table S2. Prediction accuracy of the 9 scoring functions calculated at UB. The ability of the scoring functions to predict the direction of a transformation effect (positive or negative) with and without the consideration of water is shown. Only more potent 3D-MMPs (i.e. affinity < 1 µM) were considered. Results significantly different from chance (i.e. 50%) are highlighted in blue.

scoring function[a]	3D-MMPs with $|\Delta affinity| \geq 0.5$		3D-MMPs with $|\Delta affinity| \geq 1.0$	
	w/ water	w/o water	w/ water	w/o water
Affinity dG	60.0	76.0	61.5	76.9
London dG	64.0	68.0	61.5	69.2
Alpha HB	56.0	68.0	53.9	76.9
ASE	76.0	76.0	69.23	76.9
GBVI/WSA dG	64.0	68.0	76.9	76.9
ChemScore	52.0	68.0	53.8	61.5
GOLDScore	52.0	44.0	61.5	61.5
ChemPLP	60.0	60.0	61.5	61.5
ASP	56.0	52.0	53.9	46.2
Consensus	60.0	76.0	61.5	69.2

[a]Scoring functions tested for the prediction accuracy of the transformation effect in %. The prediction accuracy of the majority vote over all scoring functions for each 3D-MMP is listed as 'Consensus'. [b]Scoring under consideration of water. [c]Scoring without consideration of water. σ_{crit}: [68.0% 69.2%] for n: [25 13]; Note that σ_{crit} is the critical value while n represents the respective subset size; The calculations of the critical value are provided in the supporting information; Values are given for subsets 5 and 6.

Table S3. Prediction accuracy of the 9 scoring functions calculated at UB after geometry-optimization. The ability of the scoring functions to predict the direction of a transformation effect (positive or negative) with and without the consideration of water is shown. Results significantly different from chance (i.e. 50%) are highlighted in blue.

scoring function[a]	3D-MMPs with $|\Delta affinity| \geq 0.5$		3D-MMPs with $|\Delta affinity| \geq 1.0$		3D-MMPs with $|\Delta affinity| \geq 2.0$	
	w/ water	w/o water	w/ water	w/o water	w/ water	w/o water
Affinity dG	41.4	50.0	38.5	48.7	53.3	40.0
London dG	44.8	58.6	46.2	64.1	66.7	66.7
Alpha HB	53.4	60.3	59.0	64.1	80.0	73.3
ASE	56.9	62.1	53.8	59.0	60.0	53.3
GBVI/WSA dG	48.3	50.0	38.5	46.2	46.7	40.0
ChemScore	41.4	43.1	41.0	46.2	46.7	46.7
GoldScore	46.6	43.1	43.6	38.5	66.7	53.3
ChemPLP	41.4	51.7	43.6	51.3	60.0	66.7
ASP	43.1	43.1	38.5	43.6	66.7	53.3
Consensus	46.6	53.4	43.6	51.3	66.7	53.3

[a]Scoring functions tested for the prediction accuracy of the transformation effect in %. The prediction accuracy of the majority vote over all scoring functions for each 3D-MMP is listed as 'Consensus'. [b]Scoring under consideration of water. [c]Scoring without consideration of water. σ_{crit}: [58.6% 60.3% 64.1% 73.3%] for n: [99 58 39 15]; Note that σ_{crit} is the critical value while n represents the respective subset size; The calculations of the critical value are provided in the supporting information; Values are given for subsets 1 to 3.

Table S4. Prediction accuracy of the 9 scoring functions calculated at UB after geometry-optimization. The ability of the scoring functions to predict the direction of a transformation effect (positive or negative) with and without the consideration of water is shown. Only more potent 3D-MMPs (i.e. affinity < 1 µM) were considered. Results significantly different from chance (i.e. 50%) are highlighted in blue.

scoring function[a]	3D-MMPs with |Δaffinity| ≥ 0.5		3D-MMPs with |Δaffinity| ≥ 1.0	
	w/ water	w/o water	w/ water	w/o water
Affinity dG	40.0	52.0	46.2	53.8
London dG	48.0	64.0	53.8	76.9
Alpha HB	64.0	68.0	76.9	69.2
ASE	68.0	76.0	69.2	84.6
GBVI/WSA dG	52.0	52.0	53.8	61.5
ChemScore	52.0	48.0	61.5	61.5
GOLDScore	52.0	44.0	53.8	46.2
ChemPLP	48.0	52.0	53.8	53.8
ASP	48.0	44.0	38.5	46.2
Consensus	52.0	56.0	53.8	61.5

[a]Scoring functions tested for the prediction accuracy of the transformation effect in %. The prediction accuracy of the majority vote over all scoring functions for each 3D-MMP is listed as 'Consensus'. [b]Scoring under consideration of water. [c]Scoring without consideration of water. σ_{crit}: [68.0% 69.2%] for n: [25 13]; Note that σ_{crit} is the critical value while n represents the respective subset size; The calculations of the critical value are provided in the supporting information; Values are given for subsets 5 and 6.

Table S5. Resolution, R_{free} and R_{work} values for the 99 3D-MMPS. Collected from the PDB.[21]

ID_pair (L/R)	Resolution L	R_{free} L	R_{work} L	Resolution R	R_{free} R	R_{work} R
3HVH_3HVJ	1,30	0,153	0,130	1,79	0,235	0,183
3OE4_3OZT	1,49	0,203	0,178	1,48	0,224	0,187
3OZS_3OZT	1,44	0,209	0,180	1,48	0,224	0,187
3SV2_3QX5	1,30	0,165	0,140	1,35	0,156	0,132
2ZDA_3SI4	1,73	0,228	0,172	1,27	0,159	0,137
1QBV_3SV2	1,80	observed 0,193		1,30	0,165	0,140
3QU0_3QXP	1,95	0,251	0,200	1,75	0,254	0,214
3R9H_3QXP	2,10	0,259	0,214	1,75	0,254	0,214
2VTP_2VTT	2,15	0,247	0,186	1,68	0,227	0,199
4JQ7_4JR3	2,73	0,237	0,207	2,70	0,248	0,213
4JR3_4JQ8	2,70	0,248	0,213	2,83	0,232	0,183
4JRV_4JQ8	2,80	0,227	0,193	2,83	0,232	0,183
4C38_4C37	1,58	0,178	0,153	1,70	0,179	0,155
2UW3_2UW4	2,19	0,252	0,187	2,00	0,274	0,216
2OH0_2OJF	2,20	0,320	0,273	2,10	0,290	0,265
3SWW_3SX4	2,00	0,234	0,197	2,60	0,275	0,203
3OC0_3KWF	2,70	0,286	0,236	2,40	0,246	0,200
4LKO_4JH0	2,43	0,263	0,226	2,35	0,272	0,243
2XPK_2J62	2,40	0,242	0,196	2,26	0,219	0,179
2WB5_2J62	2,31	0,237	0,186	2,26	0,219	0,179
2WB5_2XPK	2,31	0,237	0,186	2,40	0,242	0,196
2CES_2J7E	2,15	0,247	0,192	2,19	0,252	0,185
1OIF_2J75	2,12	0,257	0,199	1,85	0,243	0,191
2J7G_2J7E	1,91	0,225	0,187	2,19	0,252	0,185
3EJQ_3EJR	1,45	0,200	0,166	1,27	0,173	0,148
3DX1_2F7O	1,21	0,163	0,127	1,43	0,235	0,206
2F18_2F1B	1,30	0,180	0,168	1,45	0,194	0,173
4H1E_4H3I	1,90	0,297	0,26	1,96	0,254	0,213
4I0F_4I1C	1,80	0,266	0,208	2,00	0,262	0,207
4JP9_4JPC	1,80	0,221	0,187	1,80	0,210	0,185
3UO5_3UP2	2,70	0,273	0,217	2,30	0,249	0,206
4DEA_3UP7	2,45	0,262	0,218	3,05	0,292	0,233
3UNZ_3UOJ	2,80	0,278	0,231	2,90	0,274	0,227
2ONZ_2OBF	2,80	0,264	0,216	2,30	0,267	0,217
3KR0_3KR1	2,60	0,257	0,217	2,30	0,249	0,218
1N7J_1HNN	2,70	0,268	0,232	2,40	0,273	0,230
3GE7_3EOS	1,50	observed 0,162		1,78	observed 0,173	
1S39_1S38	1,95	0,242	0,209	1,81	0,222	0,197

3V0Y_3RR4	No ED available. Replaced by PDB ID 4Q4R			1,68	0,200	0,159
1LOQ_3WJW	1,50	0,198	0,173	1,59	0,186	0,164
3G1V_1LOR	1,30	0,211	0,193	1,60	0,196	0,173
3G1V_1KM3	1,30	0,211	0,193	1,50	0,192	0,162
2VCJ_2VCI	2,50	0,305	0,221	2,00	0,278	0,207
2XHX_2XHT	2,80	0,407	0,244	2,27	0,297	0,225
2YI0_2YI7	1,60	0,234	0,197	1,40	0,196	0,175
2XBX_2XBW	1,85	0,235	0,195	1,72	0,218	0,192
2UWO_2UWP	1,75	0,254	0,199	1,75	0,212	0,185
2JKH_2Y5F	1,25	0,221	0,195	1,29	0,175	0,138
4DE3_4DDY	1,44	0,206	0,163	1,36	0,205	0,171
4DE2_4DDY	1,40	0,194	0,154	1,36	0,205	0,171
3G35_4DE3	1,41	0,182	0,155	1,44	0,206	0,163
1F8C_2QWE	1,70	0,216	0,178	2,00	observed 0,149	
1F8E_1F8C	1,40	0,221	0,193	1,70	0,216	0,178
1F8D_1F8B	1,40	0,231	0,201	1,80	0,214	0,166
3O9A_3O9D	1,90	0,216	0,179	1,85	0,226	0,174
3O9B_3O9A	1,50	0,189	0,165	1,90	0,216	0,179
4DJR_3O9D	1,55	0,196	0,170	1,85	0,226	0,174
3IOC_3IOD	2,50	0,261	0,162	1,75	0,207	0,169
3IUB_3IUE	1,50	0,209	0,177	1,73	0,208	0,172
3COY_3COW	2,03	0,221	0,166	1,80	0,209	0,160
3NX7_3F15	1,80	0,200	0,162	1,70	0,190	0,171
3LKA_3LK8	1,80	0,210	0,169	1,80	0,200	0,168
3LK8_3F15	1,80	0,200	0,168	1,70	0,190	0,171
2ZFS_2ZQ2	1,51	0,191	0,133	1,40	0,162	0,116
1O35_1O3J	1,41	0,198	0,164	1,40	0,198	0,188
1TNK_1TNL	1,80	observed 0,171		1,90	observed 0,164	
3E6K_3LP4	2,10	0,245	0,164	1,90	0,204	0,155
3F80_2AEB	1,60	0,184	0,147	1,29	observed 0,165	
3SJT_3SKK	1,60	0,163	0,129	1,70	0,178	0,136
1Q6J_1Q6M	2,20	0,245	0,215	2,20	0,246	0,210
2QBP_2NT7	2,50	0,245	0,209	2,10	0,231	0,206
2VEX_2VEW	2,20	0,261	0,208	2,00	0,239	0,201
1NVR_1NVQ	1,80	0,226	0,193	2,00	0,234	0,206
2XEZ_2XF0	2,25	0,238	0,210	2,40	0,244	0,203
2WMW_2WMX	2,43	0,250	0,229	2,45	0,244	0,219
1GI8_1GI9	1,75	0,254	0,200	1,80	0,238	0,192
1OWE_1OWH	1,60	0,236	0,210	1,61	0,265	0,211
1W0Z_1W11	1,90	0,221	0,199	2,00	0,249	0,199
4EHV_4EH9	2,10	0,235	0,189	2,30	0,254	0,196
3NNU_3NNW	1,60	0,252	0,221	2,10	0,280	0,229

3GCU_3GCV	2,40	0,227	0,177	1,89	0,213	0,167
3ZSQ_3ZSO	1,70	0,200	0,161	1,75	0,209	0,163
3AV9_3AVB	1,70	0,202	0,164	1,85	0,194	0,163
4CEB_3ZSW	1,75	0,198	0,169	1,80	0,206	0,174
3F3D_3F3E	2,30	0,224	0,197	1,80	0,205	0,179
3F48_3F3E	1,90	0,229	0,211	1,80	0,205	0,179
2Q72_2Q6H	1,70	0,219	0,203	1,85	0,218	0,198
1I9Q_1G48	1,80	0,240	0,183	1,86	0,239	0,178
2H15_3HKU	1,90	0,225	0,186	1,80	0,198	0,152
3IBI_3IBU	1,93	0,205	0,169	1,41	0,215	0,200
1MQH_1MQG	1,80	0,231	0,198	2,15	0,233	0,185
1MQJ_1MQI	1,65	0,229	0,208	1,35	0,218	0,200
1MQJ_1MQH	1,65	0,229	0,208	1,80	0,231	0,198
1JVU_1O0M	1,78	0,240	0,190	1,50	0,244	0,211
3DXG_3D6O	1,39	0,254	0,208	1,58	0,227	0,186
1O0H_1AFK	1,20	0,221	0,190	1,70	0,266	0,211
3MRT_3MS2	1,98	0,216	0,181	2,10	0,223	0,183
4EL5_4EJ2	2,00	0,210	0,163	2,65	0,233	0,159
3SYR_3T3H	2,40	0,217	0,176	2,60	0,221	0,158

Table S6. EDIA$_m$ values for the data set of 99 3D-MMPs.[22]
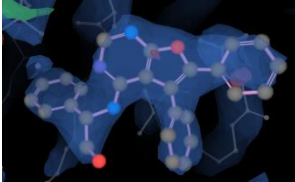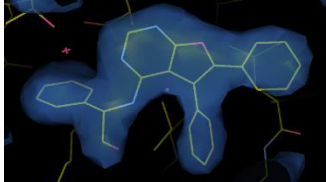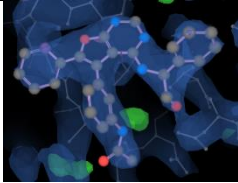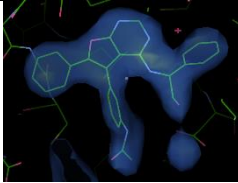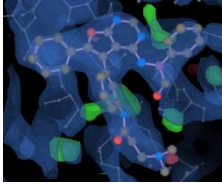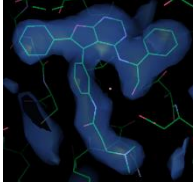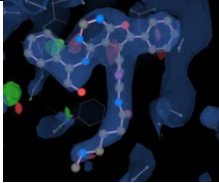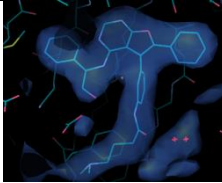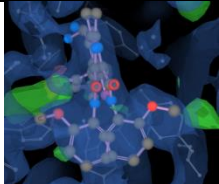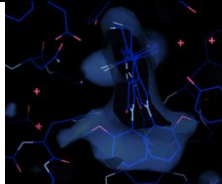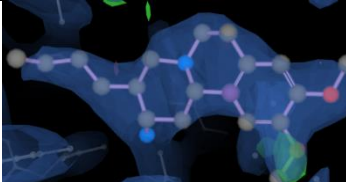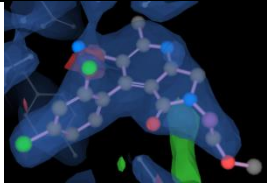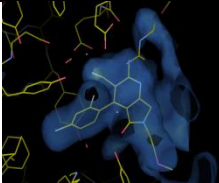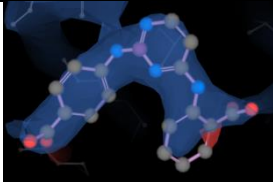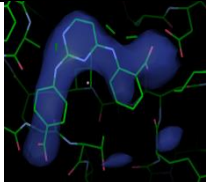
Cluster_ID	ID_pair (L/R)	EDIA$_m$_L	EDIA$_m$_R
23	3HVH_3HVJ	1,04	1,01
	3OE4_3OZT	1,06	1,03
	3OZS_3OZT	0,99	1,03
59	3SV2_3QX5	1,02	1,01
	2ZDA_3SI4	0,97	0,91
	1QBV_3SV2	No ED available[1]	1,02
83	3QU0_3QXP	0,99	1,02
	3R9H_3QXP	0,86	1,02
	2VTP_2VTT	0,84	1,02
156	4JQ7_4JR3	0,67	0,71
	4JR3_4JQ8	0,71	0,78
	4JRV_4JQ8	0,77	0,78
167	4C38_4C37	1,03	1,03
	2UW3_2UW4	0,98	0,87
	2OH0_2OJF	No ED available[1]	No ED available[1]
194	3SWW_3SX4	0,98	0,62
	3OC0_3KWF	0,64	0,85
	4LKO_4JH0	0,73	0,90
324	2XPK_2J62	0,82	0,91
	2WB5_2J62	0,89	0,91
	2WB5_2XPK	0,89	0,98
325	2CES_2J7E	0,97	0,90
	1OIF_2J75	1,00	1,07
	2J7G_2J7E	0,92	0,90
441	3EJQ_3EJR	1,00	0,97
	3DX1_2F7O	0,99	1,00
	2F18_2F1B	0,93	0,92
466	4H1E_4H3I	0,96	0,98
	4I0F_4I1C	1,02	0,98
	4JP9_4JPC	0,99	0,95
487	3UO5_3UP2	0,80	0,96
	4DEA_3UP7	0,97	0,55
	3UNZ_3UOJ	0,80	0,64
518	2ONZ_2OBF	0,83	0,99
	3KR0_3KR1	0,87	0,94
	1N7J_1HNN	0,68	0,95
686	3GE7_3EOS	0,88	1,02
	1S39_1S38	0,99	0,93
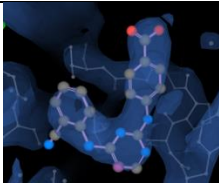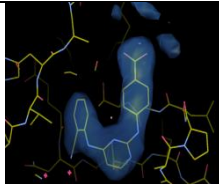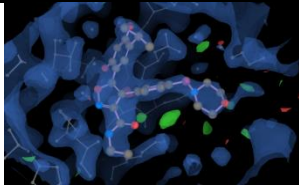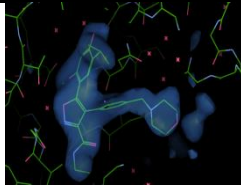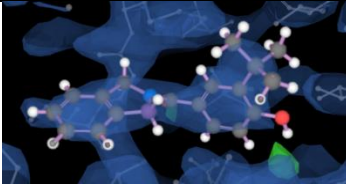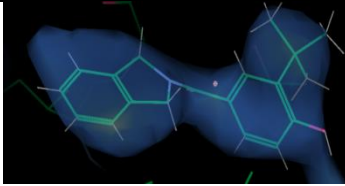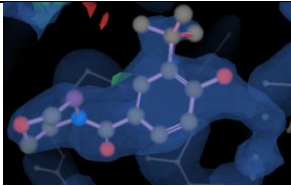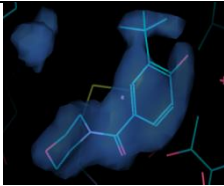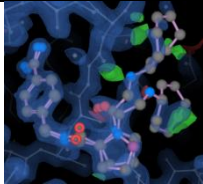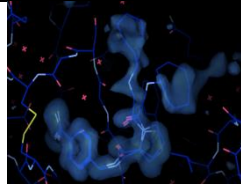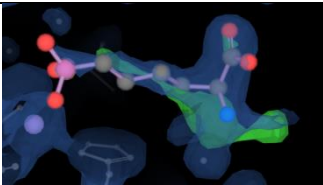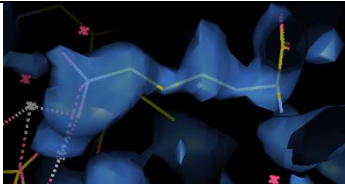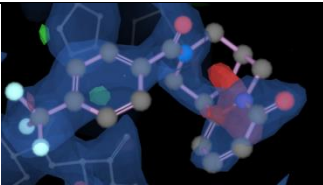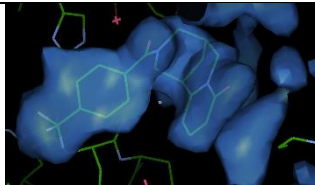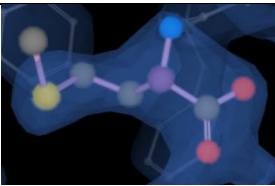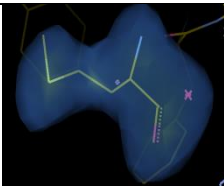
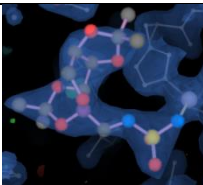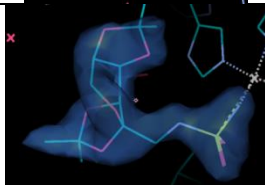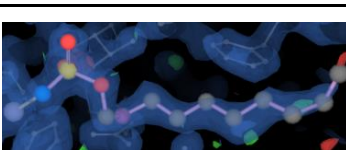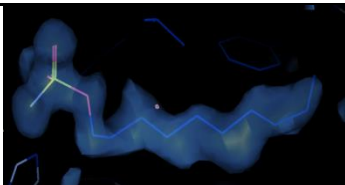|			
	3V0Y_3RR4	No ED available. Replaced by PDB ID 4Q4R	1,02
710	1LOQ_3WJW	1,04	1,06
	3G1V_1LOR	1,01	1,04
	3G1V_1KM3	1,01	No ED available[1]
745	2VCJ_2VCI	0,93	0,78
	2XHX_2XHT	0,68	0,52
	2YI0_2YI7	1,05	1,08
790	2XBX_2XBW	0,97	1,01
	2UWO_2UWP	0,96	0,93
	2JKH_2Y5F	0,92	0,91
806	4DE3_4DDY	0,94	0,90
	4DE2_4DDY	0,93	0,90
	3G35_4DE3	1,01	0,94
810	1F8C_2QWE	1,04	No ED available[1]
	1F8E_1F8C	1,01	1,04
	1F8D_1F8B	1,06	1,03
812	3O9A_3O9D	0,99	1,02
	3O9B_3O9A	1,03	0,99
	4DJR_3O9D	0,99	1,02
873	3IOC_3IOD	0,81	0,80
	3IUB_3IUE	0,93	0,96
	3COY_3COW	1,00	1,03
900	3NX7_3F15	0,94	0,93
	3LKA_3LK8	0,82	0,93
	3LK8_3F15	0,93	0,93
914	2ZFS_2ZQ2	0,98	0,37
	1O35_1O3J	1,00	0,81
	1TNK_1TNL	No ED available[1]	No ED available[1]
929	3E6K_3LP4	0,64	0,86
	3F80_2AEB	0,97	No ED available[1]
	3SJT_3SKK	0,93	1,02
942	1Q6J_1Q6M	1,01	1,03
	2QBP_2NT7	0,86	No ED available[1]
	2VEX_2VEW	0,91	0,87
975	1NVR_1NVQ	1,04	1,02
	2XEZ_2XF0	0,94	0,82
	2WMW_2WMX	0,81	0,78
979	1GI8_1GI9	0,98	0,91
	1OWE_1OWH	0,95	0,89
	1W0Z_1W11	No ED available[1]	No ED available[1]
1024	4EHV_4EH9	0,98	0,67
	3NNU_3NNW	0,97	1,03

	3GCU_3GCV	0,98	0,94
1025	3ZSQ_3ZSO	1,02	0,83
	3AV9_3AVB	No ED available[1]	No ED available[1]
	4CEB_3ZSW	1,00	0,91
1050	3F3D_3F3E	0,79	1,07
	3F48_3F3E	1,02	1,07
	2Q72_2Q6H	0,98	0,84
1051	1I9Q_1G48	No ED available[1]	No ED available[1]
	2H15_3HKU	0,56	0,97
	3IBI_3IBU	0,90	0,72
1059	1MQH_1MQG	No ED available[1]	No ED available[1]
	1MQJ_1MQI	No ED available[1]	No ED available[1]
	1MQJ_1MQH	No ED available[1]	No ED available[1]
1072	1JVU_1O0M	No ED available[1]	1,00
	3DXG_3D6O	0,61	0,29
	1O0H_1AFK	1,02	No ED available[1]
1081	3MRT_3MS2	1,03	0,83
	4EL5_4EJ2	1,04	0,27
	3SYR_3T3H	0,96	0,87

[1]No electron density available. Prior to February 1, 2008, it was not mandatory to deposit structure factor amplitudes/intensities for crystal structures for PDB deposition. (http://www.rcsb.org/pdb/static.do?p=general_information/news_publications /news/news_2007.html#20071204)

Table S7. Electron density and polder maps for structures with EDIA$_m$ values smaller than 0.8.[22]

PDB ID	Resolution	EDIA$_m$	Electron density map[a]	Polder map[b]
4JQ7	2.73	0.67		
4JR3	2.7	0.71		
4JQ8	2.38	0.78		
4JRV	2.8	0.77		
3SX4	2.6	0.62		
3OC0	2.7	0.64		
4LKO	2.4	0.38		
3UP7	3.05	0.55		

3UOJ	2.9	0.64		
2VCI	2.0	0.78		
2XHX	2.8	0.68		
2XHT	2.27	0.52		
2ZQ2	1.4	0.37		
3E6K	2.1	0.64		
4EH9	2.1	0.67		
3F3D	2.3	0.79		
2H15	1.9	0.56		
3IBU	1.4	0.72		

^aElectron density map image from http://www.ebi.ac.uk/pdbe/eds. ^bPolder maps generated with Phenix and visualised with WinCoot[23].
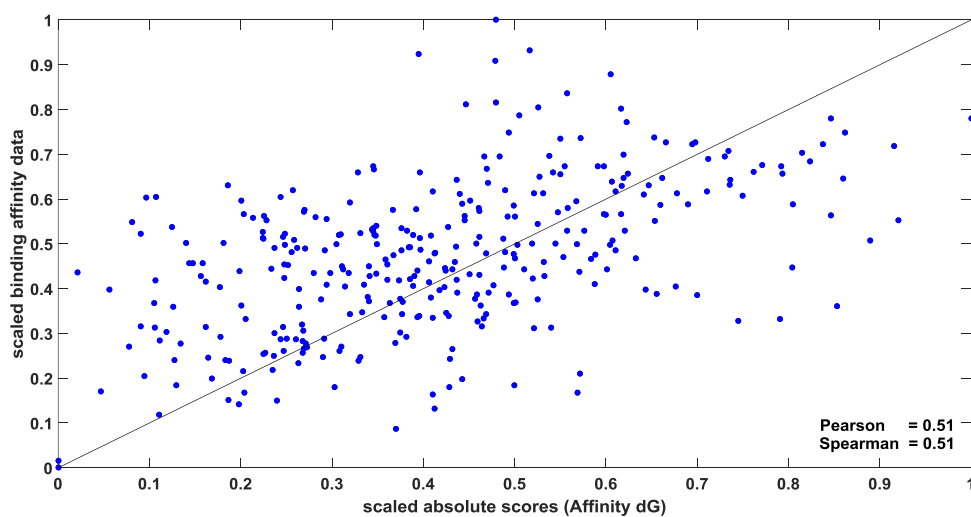
A
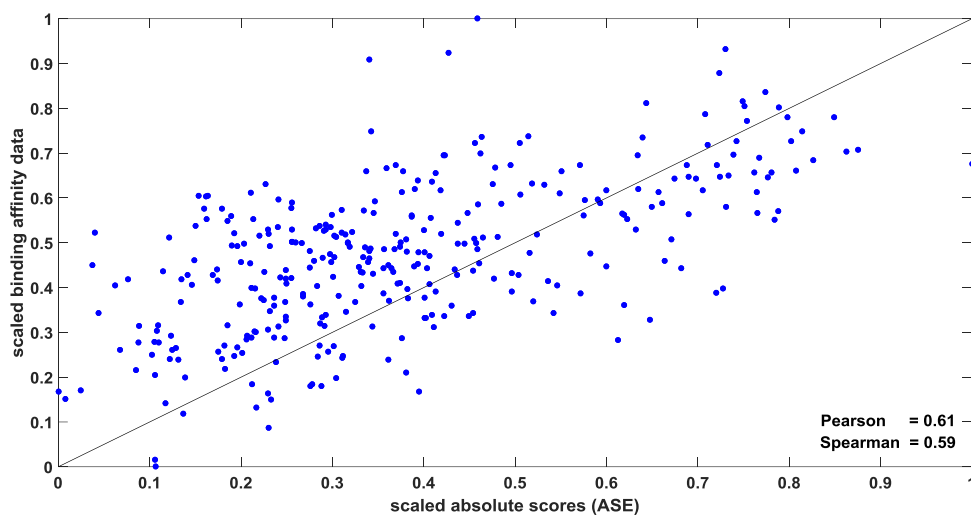
B

Figure S1. Scatter plots displaying the correlation between the scaled binding affinity data for the 332 energy-optimized complexes of the CSAR-NRC data set, excluding the protein-ligand complexes of Factor Xa and the corresponding scores of ASE (A) and Affinity dG (B). The Pearson and Spearman correlation coefficient of both scoring functions are given in the figure.
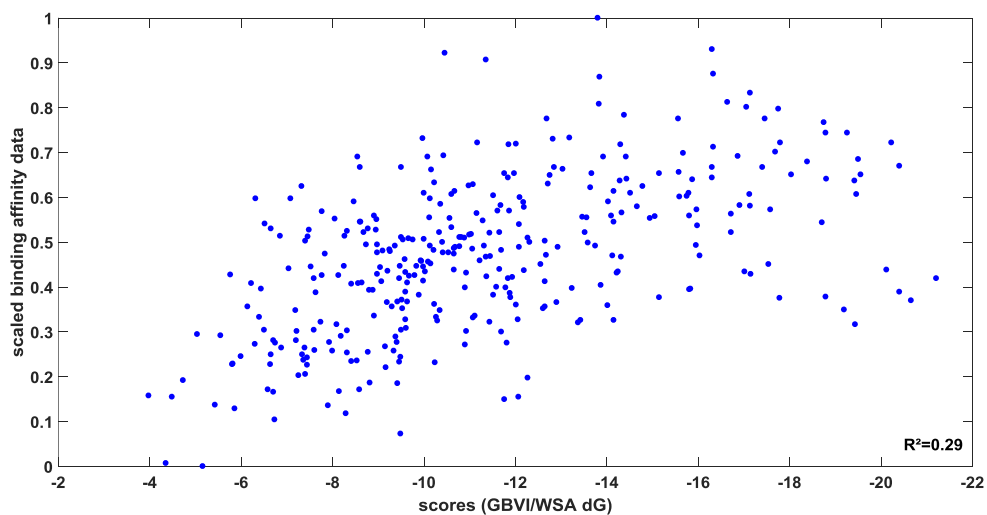
Figure S2. Scatter plot displaying the correlation between the scaled binding affinity data for the 343 energy-optimized complexes of the entire CSAR-NRC data set and the corresponding scores of GBVI/WSA dG. The coefficient of determination R^2 is given in the figure.

Critical values for statistical significance of the prediction accuracy using Δscore to predict Δaffinity

Subset	n	σ_{crit}
	99	58 (58.6%)
1	58	35 (60.3%)
2	39	25 (64.1%)
3	15	11 (73.3%)
4	54	33 (61.1%)
5	25	17 (68.0%)
6	13	9 (69.2%)

n : number of objects in the corresponding subset

σ_{crit} : critical value that the prediction accuracy is considered to be significantly different from chance (i.e. 50%) based on the 95th percentile ($\alpha = 0.05$; one-sided)

(1)   Chemical Computing Group Inc. Molecular Operating Environment (MOE), 2014.09. *Molecular Operating Environment (MOE), 2014.09*. 1010 Sherbrooke St. West, Suite #910, QC, Canada, H3A 2R7 2014.

(2)   Halgren, T. A. Merck Molecular Force Field. I. Basis, Form, Scope, Parameterization, and Performance of MMFF94. *J. Comput. Chem.* **1996**, *17*, 490–519.

(3)   Weiner, P. K.; Kollman, P. A. AMBER: Assisted Model Building with Energy Refinement. A General Program for Modeling Molecules and Their Interactions. *J. Comput. Chem.* **1981**, *2*, 287–303.

(4)   Weiner, S. J.; Kollman, P. A.; Case, D. A. A New Force Field for Molecular Mechanical Simulation of Nucleic Acids and Proteins. *J. Am. Chem. Soc.* **1984**, *106*, 765–784.

(5)   Weiner, S. J.; Kollman, P. A.; Nguyen, D. T.; Case, D. A. An All Atom Force Field for Simulations of Proteins and Nucleic Acids. *J. Comput. Chem.* **1986**, *7*, 230–252.

(6)   Naïm, M.; Bhat, S.; Rankin, K. Solvated Interaction Energy (SIE) for Scoring Protein-Ligand Binding Affinities. 1. Exploring the Parameter Space. *J. Chem. Inf. Model.* **2007**, 122–133.

(7)   Jones, G.; Willett, P.; Glen, R. C.; Leach, A. R.; Taylor, R. Development and Validation of a Genetic Algorithm for Flexible Docking. *J. Mol. Biol.* **1997**, *267* (3), 727–748.

(8)   Jones, G.; Willett, P.; Glen, R. C. Molecular Recognition of Receptor Sites Using a Genetic Algorithm with a Description of Desolvation. *J Mol Biol* **1995**, *245*, 43–53 ST–Molecular recognition of receptor site.

(9)   Verdonk, M. L.; Cole, J. C.; Hartshorn, M. J.; Murray, C. W.; Taylor, R. D. Improved Protein – Ligand Docking Using GOLD. *Proteins Struct. Funct. Bioinforma.* **2003**, *623* (January), 609–623.

(10)   Mooij, W. T. M.; Verdonk, M. L. General and Targeted Statistical Potentials for Protein-Ligand Interactions. *Proteins Struct. Funct. Genet.* **2005**, *61*, 272–287.

(11)   Korb, O.; Stützle, T.; Exner, T. E. Empirical Scoring Functions for Advanced Protein-Ligand Docking with PLANTS. *J. Chem. Inf. Model.* **2009**, *49*, 84–96.

(12)   Eldridge, M. D.; Murray, C. W.; Auton, T. R.; Paolini, G. V; Mee, R. P. Empirical Scoring Functions .1. The Development of a Fast Empirical Scoring Function to Estimate

the Binding Affinity of Ligands in Receptor Complexes. *J. Comput. Aided. Mol. Des.* **1997**, *11*, 425–445.

(13) Baxter, C. A.; Murray, C. W.; Clark, D. E.; Westhead, D. R.; Eldridge, M. D. Flexible Docking Using Tabu Search and an Empirical Estimate of Binding Affinity. *Proteins Struct. Funct. Genet.* **1998**, *33*, 367–382.

(14) CCDC Gold Suite 5.2.2. Cambridge, United Kingdom.

(15) Verdonk, M. L.; Berdini, V.; Hartshorn, M. J.; Mooij, W. T. M.; Murray, C. W.; Taylor, R. D.; Watson, P. Virtual Screening Using Protein-Ligand Docking: Avoiding Artificial Enrichment. *J. Chem. Inf. Comput. Sci.* **2004**, *44*, 793–806.

(16) Sanner, M. F. Python: A Programming Language for Software Integration and Development. *J. Mol. Graph. Model.* **1999**, *17*, 57–61.

(17) Huey, R.; Morris, G. M.; Olson, A. J.; Goodsell, D. S. Software News and Update a Semiempirical Free Energy Force Field with Charge-Based Desolvation. *J. Comput. Chem.* **2007**, *28*, 1145–1152.

(18) Trott, O.; Olson, A. J. Software News and Update AutoDock Vina : Improving the Speed and Accuracy of Docking with a New Scoring Function , Efficient Optimization , and Multithreading. *J. Comput. Chem.* **2010**, *31*, 455–461.

(19) Wang, R.; Liu, L.; Lai, L.; Tang, Y. SCORE: A New Empirical Method for Estimating the Binding Affinity of a Protein-Ligand Complex. *J. Mol. Model* **1998**, *4*, 379–394.

(20) Neudert, G.; Klebe, G. DSX: A Knowledge-Based Scoring Function for the Assessment of Protein-Ligand Complexes. *J. Chem. Inf. Model.* **2011**, *51*, 2731–2745.

(21) Berman, H. M.; Westbrook, J.; Feng, Z.; Gilliland, G.; Bhat, T. N.; Weissig, H.; Shindyalov, I. N.; Bourne, P. E. The Protein Data Bank. *Nucleic Acids Res.* **2000**, *28* (1), 235–242.

(22) Meyder, A.; Nittinger, E.; Lange, G.; Klein, R.; Rarey, M. Estimating Electron Density Support for Individual Atoms and Molecular Fragments in X-Ray Structures. *J. Chem. Inf. Model.* **2017**, *57* (10), 2437–2447.

(23) Emsley, P.; Lohkamp, B.; Scott, W. G.; Cowtan, K. Features and Development of Coot. *Acta Crystallogr. Sect. D Biol. Crystallogr.* **2010**, *66* (4), 486–501.